Self-Diffusion and Correlation Effects in Ordered AuZn Alloys*

D. Gupta† and D. S. Lieberman
Department of Mining, Metallurgy, and Petroleum Engineering and Materials Research Laboratory, University of Illinois at Urbana-Champaign, Urbana, Illinois 61801
(Received 15 March 1971)

Simultaneous self-diffusion measurements of Zn and Au in near-equiatomic highly ordered AuZn ($B2$ structure) single-crystal specimens having 49.0, 50.0, 51.0 at.% Zn nominal composition were made over a temperature range of 428–650 °C using Zn^{65} and Au^{195} radioactive tracers and the serial lathe sectioning technique. Employing a modified energy-discrimination method for nuclear counting, it was possible to measure the ratio of diffusivities D_{Zn}/D_{Au}—in addition to their individual values—following simultaneous diffusion of the two radioactive tracers in the same specimen. The diffusion parameters Q and D_0 and the entropy of activation factor were computed in the composition range studied and compared with the corresponding quantities in the disordered Zn-base monovalent alloys ($A2$ structure). The magnitude of the ratio of the correlation factors in ordered and disordered phases was found to be consistent with the correlated six-atom-vacancy-jump diffusion mechanism in the highly ordered alloys. The self-diffusion data for Au and Zn in β'-AuZn alloys also provides strong evidence for the presence of a nonequilibrium vacancy-defect structure on the Zn-rich side of stoichiometry.

I. INTRODUCTION

A simple statistical model of diffusion in cubic materials leads to the following expression for the diffusion coefficient[1] D:

$$D = D_0 e^{-\Delta H/RT} \tag{1}$$

and

$$D_0 = \gamma a^2 \bar{\nu} f e^{\Delta S/R}, \tag{2}$$

where γ is a geometrical factor which is equal to unity for cubic lattices, a the lattice parameter, $\bar{\nu}$ the mean lattice frequency (commonly taken as the Debye frequency), ΔS and ΔH (usually denoted by Q) the entropy and enthalpy changes associated with the process, R the gas constant, and T the absolute temperature. The factor f is called the *correlation factor* and is a measure of the nonrandom character of atomic jumps; it equals 0.727 and 0.782 in bcc and fcc lattices, respectively.[2] The temperature-independent D_0 in Eq. (2) is the preexponential or frequency factor. In a perfectly ordered binary alloy AB consisting of two simple-cubic interpenetrating sublattices α and β (each occupied by atoms of one kind only), the nearest-neighbor lattice sites of one sublattice would all lie on the other, any self-diffusion process would have to be constrained to occur in such a way that the equilibrium degree of order is maintained.

In the particular case of CsCl-type alloys, a model of the correlated atom-vacancy motion—known as the Huntington-McCombie-Elcock (HME) model—has been favored on both theoretical and experimental grounds.[3–8] The proposed motion consists of (at least) six-atom-vacancy interchanges around a planar and/or "folded" {110} rhombus, as shown in Fig. 1. The "wrong configuration" caused by putting atoms on the wrong sublattice during the first three jumps is converted to a "right configuration" by the subsequent three jumps. The model permits the net diffusion of both the species in the alloy and predicts that the ratio of their diffusivities will lie in the range $\frac{1}{2}$–2 (depending on the initial position of the vacancy on one sublattice or the other) owing to geometrical considerations alone. After taking into account other contributing factors, viz., vacancy concentrations on the two sublattices n_α and n_β and the vacancy motional (saddle point) energies ΔH_{mA} and ΔH_{mB}, respectively, the ratio of the diffusion coefficients may be written

$$G = \frac{D_A}{D_B} = \frac{n_\alpha \bar{\nu}_A e^{-\Delta H_{mA}/RT} + 2n_\beta \bar{\nu}_B e^{-\Delta H_{mB}/RT}}{2n_\alpha \bar{\nu}_A e^{-\Delta H_{mA}/RT} + n_\beta \bar{\nu}_B e^{-\Delta H_{mB}/RT}}, \tag{3}$$

where $\bar{\nu}_A$ and $\bar{\nu}_B$ are the "allowed" mean lattice frequencies. Elcock[9] estimated lower and upper limits of $\frac{2}{3}$ and $\frac{3}{2}$ for G in fully ordered alloys at low temperatures ($T/T_C \leq 0.5$) if all unit processes other than the six-jump were ignored.

Experimental values of the ratios of diffusivities in[5] β'-AuCd (β' designates $B2$ structure) alloys are in excellent agreement with this prediction. An interesting feature of the six-jump cycle is that it predicts that an excess of vacancies on one sublattice (for example, α) will enhance the diffusivity of the B atoms on β both absolutely and relatively, that is $D_B > D_A$. This effect was observed and existence of a vacancy-defect structure inferred in the Cd side only. Recent work of Fishman *et al.*[10] on the isotope-effect measurement of Fe in equiatomic FeCo has provided further evidence in favor of the six-jump-cycle diffusion mechanism. The

strength of the isotope effect E_α is related to f_α through the expression $E_\alpha = f_\alpha(\Delta K)$, where ΔK is a fraction of the translational kinetic energy possessed by the jumping atom as it crosses the saddle point and is dependent on the stiffness of the lattice.[11] It was argued[10] that in FeCo ΔK should be insensitive to the degree of order and, hence, the entire observed change below the ordering temperature $T_C = 730$ °C of almost an order of magnitude in E_{Fe} was attributed to a change in mechanism from the relatively uncorrelated vacancy motion in the disordered phase ($f_{Fe} \simeq 0.73$) to a highly correlated motion in the ordered phase. The observed f_{Fe} (ordered) is approximately equal to 0.1; if f_{Fe} (ordered) is approximately equal to $[f_{Fe}$ (disordered)$]^\kappa$ as implied by the HME model, then $\kappa \cong 6$, the same as the number of jumps in this model.

Monte Carlo computations by Beeler and Delaney[12] on a planar lattice suggest that 90% of the vacancy jumps get consumed in retracted excursions and only about 1% are actually completed in the HME cycle. However, when the long-range order parameter S is approximately unity, net transport is only possible by the HME loops. The work of Fishman *et al.*[10] and Beeler and Delaney,[12] therefore, suggest that diffusion by the correlated six-jump cycles is a very inefficient process and consequently the frequency factor D_0 [Eq. (2)] should be substantially lower in an ordered alloy than its counterpart in a fully disordered alloy. Further, if factors other than f in Eq. (2), i.e., $a^2 \bar{\nu} e^{\Delta S/R}$ can be determined independently, a direct comparison of the correlation factors in the two phases may be possible without having to carry out the difficult isotope-effect measurements. Such an approach has not been possible thus far; only marked deviations from the high-temperature diffusion coefficients extrapolated below T_C in Arrhenius plots have been treated (rather qualitatively) in CuZn[13] and FeCo.[10]

The object of this investigation was to determine the diffusion parameters Q and D_0 in a highly ordered alloy system, to compare them with the corresponding quantities in fully disordered systems in an effort to ascertain the relative magnitudes of the correlation effects in the two cases, and to see whether the results for the ordered alloy substantiate the six-atom-vacancy-jump mechanism. The AuZn system is well suited for this study since it has a stable β' phase extending from about 45.0 to 53.0 at.% Zn at room temperature which becomes wider at elevated temperatures.[14] Fortunately β'-AuZn alloys do not exhibit any solid-state transformation down to rather low temperatures and, hence, present no experimental difficulties for specimen preparation or serial lathe sectioning for profiling the tracer penetration, as did the AuCd system.[5] Further, good radioisotopes of Au and Zn are available for tracer diffusion work.

AuZn belongs to the family of noble-metal Hume-Rothery electron compounds (with the valence electron-to-atom ratio of $\frac{3}{2}$) which includes β'-AuCd, β'-AgMg, β/β'-CuZn, and β-AgZn. In the equiatomic AuZn alloy, the long-range order (LRO) parameter S (inferred from recent x-ray measurements[15]) remains as high as 0.96 even at 650 °C (only 75 °C below its melting point). Hence, in the apparent absence of a fully disordered phase, diffusion parameters were measured as a function of temperature and composition to observe any changes in Q and D_0 and to study the effects of small departures from exact stoichiometry and LRO on the number and distribution of defects (vacancies and antistructure or "wrong" atoms) on the two sublattices. These diffusion parameters measured in single-crystal alloy specimens of nominal composition 49.0, 50.0, and 51.0 at.% Zn were then compared with the published diffusion data in some of the other β Hume-Rothery alloys[5,6,13,16–21] mentioned above. As seen from Eq. (3), the ratio of diffusivities (in addition to their individual values) is essential in order to differentiate among diffusion mechanisms which may be operative in the ordered alloy. A precise measurement of this quantity is only possible when the two radiotracers are diffused *simultaneously* in the same specimen (as first done in AuCd[5]) for only then do identical conditions of composition, temperature, dislocation configuration, etc., prevail during diffusion and are the errors during the subsequent sectioning and counting operations the same. By a modified energy discrimination counting technique, it was possible to make simultaneous diffusion measurements of Au^{195} and Zn^{65} tracers and, hence, a direct determination of D_{Zn}, D_{Au}, and D_{Zn}/D_{Au} at several temperatures and compositions.

II. EXPERIMENTAL PROCEDURES

A. Specimen Preparation, Diffusion of Tracers, and Sectioning

A general description of the experimental pro-

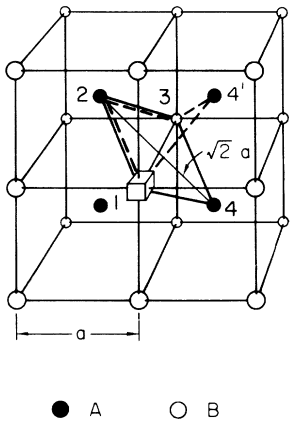

FIG. 1. Six-jump sequence diffusion paths which maintain order in CsCl-type lattice: (1) planar rhombus 12341-solid line; (2) folded rhombus 1234'1-dashed line.

cedures for the preparation of CsCl-type alloy diffusion specimens, tagging of the radioactive tracers, and diffusion annealing has been given in detail by the authors elsewhere.[5,8,10] The starting metals for the β'-phase AuZn alloys used in this investigation were 99.999+% purity Au and Zn.[22] Since quartz could not be used as a container because of its chemical reaction with Zn, alumina crucibles ($\frac{3}{8}$ in. diam) were used which were previously coated with graphite-Dag and baked in a vacuum at 300 °C. After charging a crucible with the metals, its top was capped with a graphite plug and the assembly encapsulated in quartz under a vacuum of 10^{-5} Torr. The metals were fused and mixed at 800 °C, and alloy single crystals grown in a vertical Bridgman-type furnace.

All single crystals were homogenized for 72 h at 700 °C. Specimens of $\frac{3}{8}\times\frac{3}{8}$ in. diam were spark cut from the long single crystals, lapped, polished, etched in 50% aqua regia at 50 °C, and annealed a second time prior to the diffusion of tracers. Only crystals found to be good after metallographic and x-ray examination were used. At least six specimens for each of the 49.0, 50.0, and 51.0 at.% Zn nominal compositions were thus obtained. Following analyses,[23] the temperature and compositional variation of diffusivity could be fully determined.

Carrier-free Au^{195} (180 day, 0.067-MeV γ), and high-specific-activity Zn^{65} (248 day, 1.1-MeV γ, and 0.33-MeV β^+) radioactive isotopes[24] were electroplated (one over the other) onto the flat surfaces of the specimens. The thin-layer geometry was maintained. The specimens were annealed in quartz capsules under $\frac{1}{3}$ atm of pure argon with flat quartz spacers on their faces. "Warm-up time" corrections were made for short diffusion anneals; the sharp cutoff was obtained by quenching the capsules in water.

Serial lathe sectioning was used to profile the penetration of the radioisotopes. The penetration distance was calculated on the basis of the cumulative weights of the successive slices, diameter of the specimen, and the measured density.[25]

B. Counting

The energy-discrimination technique was used for the counting of Au^{195} (0.067-MeV γ) and Zn^{65} (1.1-MeV γ) radioactivities in the alloys following simultaneous diffusion. A two channel scintillation spectroscope was used which included a double set of linear amplifiers, pulse-height analysers and scalers, and a $\frac{1}{2}\times$2-in.-diam NaI (Tl) crystal as a detector. Separate windows for Au^{195} and Zn^{65} photons could be set for simultaneous counting. The backscatter present in Zn^{65} tracer, however, hindered direct counting of Au^{195} in the diffused sections; no such difficulty was experienced for Zn^{65} counting. Corrections for the Au^{195} counting were made by a calibration scheme. First, the backscatter of Zn^{65} at the Au^{195} window was determined in an external standard relative to its 1.1-MeV γ activity, and then it was scaled to the actual level of Zn^{65} (1.1-MeV γ) activity present in the diffused section. The resulting backscatter contribution was finally deducted from the observed counting rate at the Au^{195} (0.067-MeV γ) window to obtain net Au^{195} activity in the diffused section. In actual practice, Zn^{65} and Au^{195} standards were counted at both windows between diffusion sections; the latter being dry lathe cuttings.

The least-square values of diffusion coefficients were then computed according to the instantaneous thin planar source condition[11]

$$C=[C_0/(\pi Dt)^{1/2}]e^{-x^2/4Dt}\,, \tag{4}$$

where D is the diffusion coefficient, C the concentration of tracer at the penetration distance x and time t, and C_0 the tracer concentration at $x=0$ and $t=0$. For Au^{195} and Zn^{65} tracers diffusing simultaneously, the ratio of their isotopic activities is thus

$$\ln(C_{Au}/C_{Zn})=\text{const}+(1-D_{Zn}/D_{Au})\,x^2/4D_{Zn}t\,. \tag{5}$$

The relative rates of diffusion $(1-D_{Zn}/D_{Au})$ and, hence, the ratio D_{Zn}/D_{Au} were obtained directly as slopes of $\ln(C_{Au}/C_{Zn})$-vs-$x^2/4D_{Zn}t$ plots.

III. RESULTS

Three β'-AuZn alloys having *nominal* compositions of 49.0, 50.0, and 51.0 at.% Zn were studied at six different temperatures in the range 428–650 °C. Precise chemical analysis of the individual specimens subsequent to the diffusion runs per-

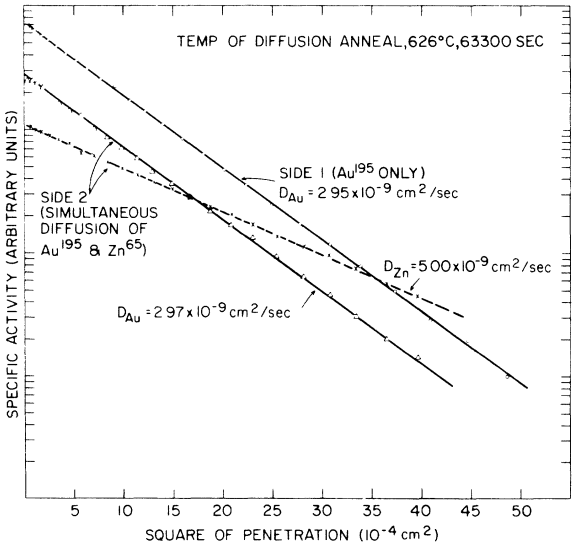

FIG. 2. Calibration for simultaneous diffusion of Au^{195} and Zn^{65} tracers in a 50:50 β'-AuZn alloy specimen.

TABLE I. Self-diffusion coefficients and the ratios (D_{Zn}/D_{Au}) in β'-AuZn alloys.

Actual comp at.% Zn ±0.02	Temp °C ±0.1	D_{Zn}(cm²/sec) ±5%	D_{Au}(cm²/sec) ±5%	D_{Zn}/D_{Au} ±5%
	49.0 at.% Zn (nominal)			
49.28	428.5	1.63×10^{-11}	2.13×10^{-11}	0.77
49.02	480.4	8.12×10^{-11}	1.05×10^{-10}	0.77
49.39	498.8	1.33×10^{-10}	1.50×10^{-10}	0.89
49.09	541.1	4.31×10^{-10}	4.84×10^{-10}	0.89
49.27	599.9	2.05×10^{-9}	1.96×10^{-9}	1.05
49.07	648.9	5.97×10^{-9}	5.55×10^{-9}	1.08
	50.0 at.% Zn (nominal)			
49.99	428.1	1.98×10^{-11}	1.84×10^{-11}	1.07
50.16	428.7	...	1.76×10^{-11}	...
49.83	464.1	...	4.79×10^{-11}	...
49.93	481.4	9.98×10^{-11}	7.25×10^{-11}	1.38
50.37	480.7	1.92×10^{-10}	1.19×10^{-10}	1.61
50.28	499.1	2.49×10^{-10}	1.61×10^{-10}	1.55
50.12	541.1	6.42×10^{-10}	4.34×10^{-10}	1.48
50.17	564.4	1.50×10^{-10}	...	...
50.21	599.9	2.83×10^{-9}	1.76×10^{-9}	1.61
49.97[a]	626.2	5.00×10^{-9}	2.95×10^{-9}	1.69
49.93	650.25	8.05×10^{-3}	5.24×10^{-9}	1.53
	51.0 at.% Zn (nominal)			
51.24	428.1	1.69×10^{-10}	9.54×10^{-11}	2.10
51.05	481.5	7.08×10^{-10}	3.08×10^{-10}	2.29
51.42	499.5	1.70×10^{-9}	4.85×10^{-10}	2.44
51.84	541.1	4.70×10^{-9}	1.46×10^{-9}	2.23
51.57	599.2	7.83×10^{-9}	3.16×10^{-9}	2.51
51.25	648.5	1.82×10^{-8}	8.22×10^{-9}	2.20

[a]Calibration point for Fig. 2.

mitted the compositional dependence of the self-diffusion parameters to be deduced in the 49–52 at.% Zn range. The indirect counting procedure mentioned above for determining the diffusion of Au^{195} was checked as follows: One side of a 49.97 at.% Zn specimen was plated with only Au^{195} isotope and the other side with both Au^{195} and Zn^{65} tracers. Following diffusion at 626.2 °C and subsequent processing, diffusivity of Zn^{65} and two diffusivities of Au^{195} were obtained—one from the side with only Au^{195} and the other from the side with both Au^{195} and Zn^{65}. As seen in Fig. 2, Au^{195} diffusion coefficients from both sides are the same within the experimental error. Typical penetration profiles were straight lines over at least two orders of magnitude and, consequently, contributions due to surface and dislocation pipe diffusion are concluded to have been negligible during these runs.

The diffusion data are summarized in Table I and displayed as functions of composition and temperature in Fig. 3. The diffusivity ratios listed therein have been computed from the slopes of the simultaneous-diffusion profiles (log ratio of specific activities of Au^{195} to Zn^{65} tracers vs $x^2/4D_{Zn}t$). A set of these profiles at 428 °C is shown in Fig. 4. The ratio D_{Zn}/D_{Au} undergoes a large change at a very slight deviation from stoichiometry, e.g., at 428 °C it changes from a value of 0.77 in 49.28 at.% Zn alloy to 2.10 in 51.24 at.% Zn alloy. It may be seen from Table I that the diffusivity ratio is also temperature sensitive but not so strongly.

Since significant composition deviations from the nominal composition were encountered among the specimens, diffusion parameters Q and D_0 at a composition were obtained by reading off diffusivities of the six isotherms (Fig. 3) and then carrying out Arrhenius-type analysis. Arrhenius plots of the interpolated diffusivities at 49.0, 50.0, and 51.0 at.% Zn compositions are shown in Fig. 5. Within the experimental errors, all of these plots are straight lines; only the one for 51.0 at.% Zn alloy shows appreciable scatter due to the strong composition dependence of diffusivities in the Zn-rich region. The activation energies and frequency factors are plotted in Fig. 6, where the vertical lines a, b, c refer to the nominal compositions, and listed in Table II. It is seen that Q and D_0 both seem to peak at about 50.0 at.% Zn—although the

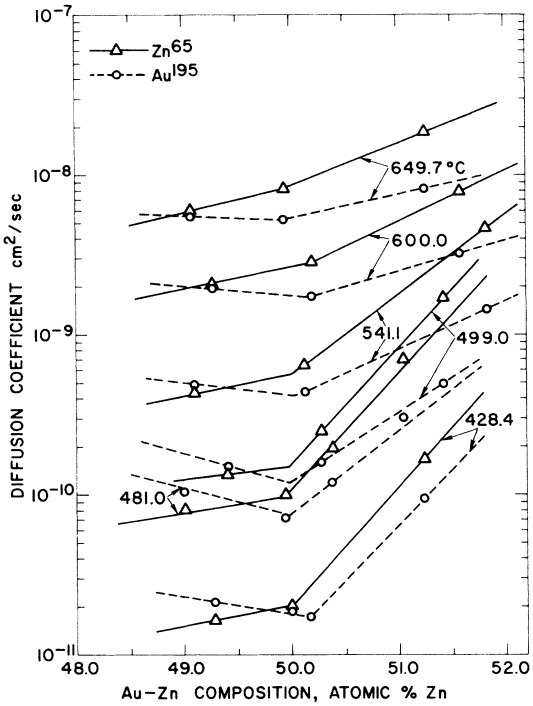

FIG. 3. Temperature and compositional dependence of diffusion coefficients of Au^{195} and Zn^{65} in β'-AuZn.

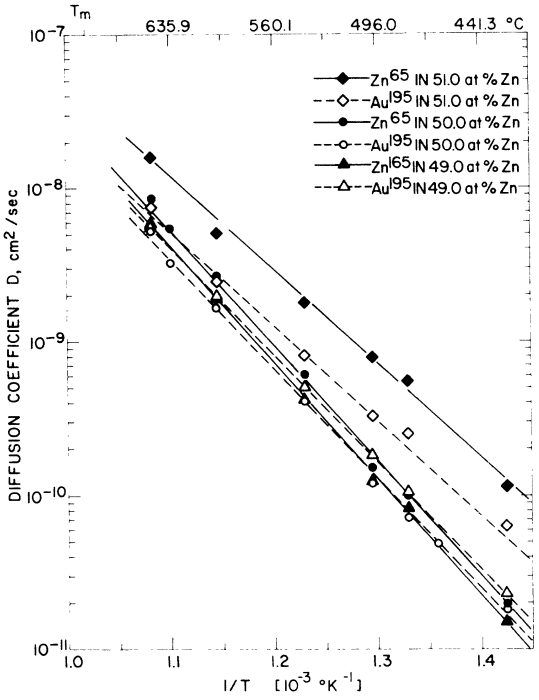

FIG. 5. Temperature variation of the diffusion coefficients in 49.0, 50.0, and 51.0 at.% Zn alloys.

drop is asymmetrical—and the changes in Q and $\log D_0$ for both the tracers appear to be parallel. To characterize these trends fully in the intervening region as well, interpolations were carried out on the six isotherms (Fig. 3) at 0.25-at.% intervals in the 48.75 and 51.75 at.% Zn composition range, and least-square values of Q and D_0 computed which are shown by circles and squares in Fig. 6. As will be seen in Sec. IV C, such an approach permitted further analysis of the diffusion parameters.

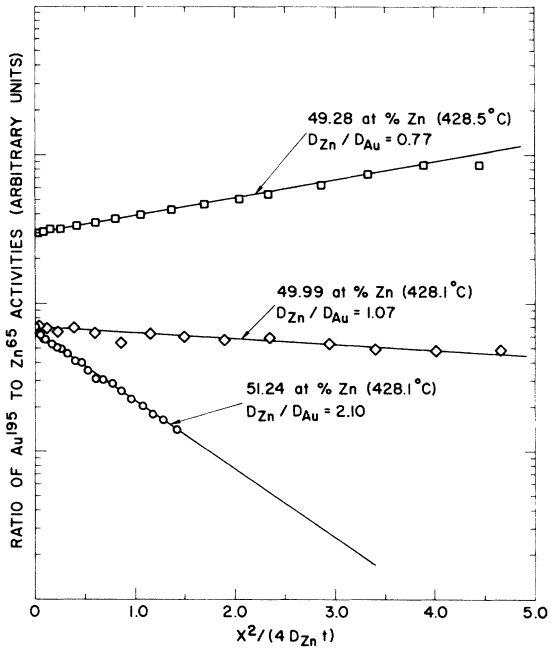

FIG. 4. Simultaneous-diffusion profiles of Au^{195} and Zn^{65} tracers.

IV. DISCUSSION

A. Temperature and Composition Dependence of Diffusion Coefficients and Ratios

The salient features of the diffusion coefficients and their ratio, listed in Table I and shown in Figs. 3 and 4, are the following: (i) The six isotherms of D_{Au} show distinct "cusps" at about 50.0 at.% Zn while the slopes of the D_{Zn} isotherms exhibit definite changes in magnitude—but no change in the sign—(also) at about 50 at.% Zn. (ii) Both D_{Au} and D_{Zn} increase very rapidly on the Zn-rich side at all temperatures with rates which increase with decreasing temperature—the rate at 428.1 °C, for example, is almost an order of magnitude larger than at 649.7 °C. (iii) The ratio of diffusivities $G = D_{Zn}/D_{Au}$ is almost temperature insensitive in the 51.0 at.% Zn specimen, more temperature dependent in the 50.0 at.% Zn alloy, and quite sensitive in the 49.0 at.% Zn alloy—in fact, $1 - D_{Zn}/D_{Au}$ changes sign at about 600 °C for this composition. (iv) G is also very composition dependent, e.g., in

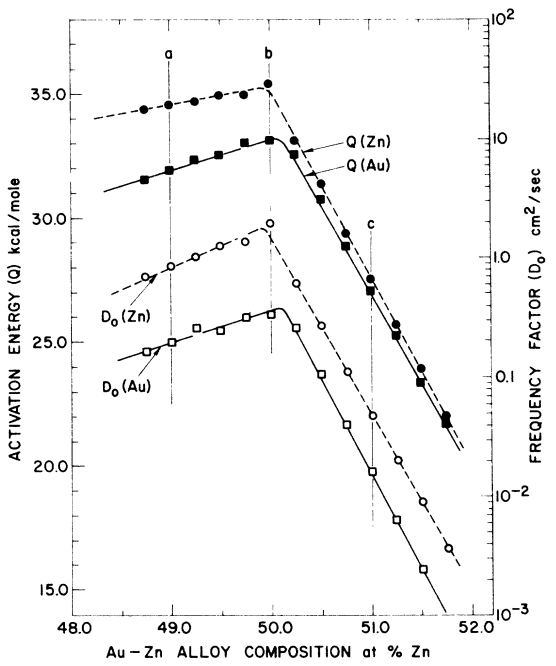

FIG. 6. Composition variation of Q and D_0 for Au^{195} and Zn^{65} tracers. The values have been obtained by interpolation on the isotherms in Fig. 3 and least-squares methods using $D = D_0\, e^{-Q/RT}$ relationship. a–c refer to the nominal compositions of the specimens used.

Fig. 4 at 428 °C it changes from 2.20 (Zn moving much faster than Au) in 51.25 at.% Zn to 0.77 (Au moving faster than Zn) in 49.28 at.% Zn; the "crossover point" is always on the Au-rich side and shifts further in that direction with increasing temperature.

The above observations are quite similar to those in AuCd[5,6] and AgMg.[20,21] Gupta *et al.*[5] accounted for all of the observations in AuCd on the basis of diffusion by HME loops and the presence of defects: antistructure or substitutional "wrong" atoms on the noble-metal-rich side and vacancies the other side of the 50:50 composition. The major difference in the AuZn data is that the upper Elcock limit of $\frac{3}{2}$ is exceeded, as seen in Table I, where the value of G is of the order of 2 in 51.0 at.% Zn specimens. The value of G is actually given by Eq. (3), and Elcock's limits are only approximations thereto. G is primarily controlled by the relative vacancy concentration factor $n \equiv n_{Zn}/n_{Au}$ on the two sublattices and only to a small extent by the energy of the configuration term $(\Delta H_{mZn} - \Delta H_{mAu})$ for an atom at a saddle point between two vacancies, one on each sublattice. According to Huntington *et al.*,[6] the term $(\Delta H_{mZn} - \Delta H_{mAu})$ may be considered almost equivalent to the difference between the self-diffusion energies $(Q_{Zn} - Q_{Au})$ and of magnitude of the ordering energy, which does not exceed $2RT$ at the temperatures of diffusion anneals.

Thus, the difference $(Q_{Zn} - Q_{Au})$ at 924 °K, the highest temperature of diffusion annealing in Table I, should not exceed 3.7 kcal/mole. It may be seen in Table II and Fig. 5 that the measured activation-energy difference $(Q_{Zn} - Q_{Au})$ lies in the range 0.5–2.9 kcal/mole and, despite its compositional dependence, remains below the quantity $2RT$ (i.e., 3.7 kcal/mole at 924 °K). Since $\bar{\nu}_{Zn}$ and $\bar{\nu}_{Au}$ may be considered equal,[5,6] Eq. (3) can be expressed as

$$G = \frac{D_{Zn}}{D_{Au}} = \frac{n + 2e^{(Q_{Zn}-Q_{Au})/RT}}{2n + e^{(Q_{Zn}-Q_{Au})/RT}} \,. \tag{6}$$

The values of the diffusivity ratio may now be estimated for the following three cases of n:

Case I. $n = 1$, i.e., when vacancies are equally probable on the two sublattices. This situation pertains to the stoichiometric alloy only and has been considered earlier in the 50% β'-AuCd alloy by Huntington *et al.*,[6] where the term $(Q_{Cd} - Q_{Au})$ was *a priori* approximated to $2RT$ yielding $D_{Cd}/D_{Au} \sim \frac{5}{3}$ in comparison to the measured average ratio of $\frac{4}{3}$. In the present case of 50% β'-AuZn alloy, the $(Q_{Zn} - Q_{Au})$ equal to 2.3 kcal/mole may be used from Table II much more effectively; the ratio G in that event falls in the range 1.45–1.60 (923–700 °K) with only slight temperature dependence. It is seen that the measured ratios of diffusivities D_{Zn}/D_{Au} in 50% β'-AuZn (Table I) also fall in this range.

Case II.. For $n \ll 1$, when vacancies on the Au sublattice outnumber the vacancies on the Zn sublattice. Physically, this case implies a vacancy-defect structure in the Zn-rich side which produces vacancies on the Au sublattice to accommo-

TABLE II. Values of the diffusion parameters in the Arrhenius relation $D = D_0\, e^{-Q/RT}$, for AuZn alloys.

	Diffusion of Zn^{65}		Diffusion of Au^{95}	
Alloy comp at.% Zn	Q Zn (kcal/mole)	D_0 Zn (cm^2/sec)	Q Au (kcal/mole)	D_0 Au (cm^2/sec)
49.0	34.6	0.84	31.9	0.19
50.0	35.4	1.93	33.1	0.33
51.0	27.5	0.047	27.0	0.016

date excess Zn atoms without diminishing the degree of LRO. The ratio of diffusivities in this event approaches the value of 2 ($G \to 2$). The effect of the unequal vacancy population is very strong and far outweighs the contribution of the configuration energy term, $0.5 < (Q_{Zn} - Q_{Au}) < 3.0$ kcal/mole. The Elcock's limit of $\frac{3}{2}$ is only an intermediate case and, depending on the magnitude of n when it is less than 1, can be exceeded easily. This also explains the observation No. ii in the Fig. 3 and predicts that Zn and Au diffusivities increase both absolutely and relatively in the Zn-rich side because of the presence of the vacancy-defect structure and diffusion taking place through the HME cycles between the two sublattices.

Case III. For $n \gg 1$, when the vacancy population on the Zn sublattice is much more than on the Au sublattice. This is exactly the opposite to the case II, i.e., if the vacancy defect structure were to be found on the Zn sublattice in the Au-rich alloy, G should approach 0.5 ($G \to 0.5$). The behavior of the Zn and Au diffusivities in the Au-rich side, however, is markedly different than the preceding case of the Zn-rich AuZn alloys. The absence of the "cusps" in the D_{Zn} data (Fig. 3) manifests itself in a *decrease* rather than an *increase*, even though D_{Au} increases as the alloy deviates more and more in the Au-rich side. Although the precise explanation for this difference is expected to emerge from the discussion in Secs. IV B and IV C, it may be mentioned here that β'-AuZn in particular—and CsCl-type alloys in general—do not appear to possess vacancy-defect structures in the noble-metal-rich side of stoichiometry and case III, may not represent any real physical situation.

B. Composition Dependence of Self-Diffusion Activation Energy Q

The variation of the activation energies for self-diffusion of Au and Zn tracers with composition shown in Fig. 6 is very similar, in extent and character, to the behavior of β'-AuCd.[5] The decrease in Q in the Au-rich β'-AuZn alloys is very gentle at a rate of about 4% for 1-at.% composition change from the peak position; the corresponding rates in β'-AuCd and β'-AgMg[20] are 2–4% in the noble-metal-rich side. Such a small change in the diffusional activation energy is actually in agreement with the quasichemical calculations[20] of Domian and Aaronson when only substitutional defects are assumed in the off-stoichiometric alloys and diffusion takes place by the HME loops. Hence this observation constitutes strong evidence for the presence of antistructure (substitutional) defects in the Au-rich AuZn alloys. The situation is, however, markedly different in the Zn- and Cd-rich alloys of β'-AuZn and AuCd systems where Q changes at rates of about 20% and 10%, respectively, per at.% deviation from the stoichiometry. This sharp drop in the measured diffusional activation energy ties in well with the presence of vacancy-defect structure in the Zn-rich alloys. The intrinsic vacancies (the nonequilibrium vacancies of off-stoichiometric origin of the order 1-at.% concentration) seem to overwhelm the extrinsic vacancy (equilibrium) formation process which are far fewer in number having concentration of only ~0.05%.[26] Consequently, the energy-of-formation term in the diffusion energy $Q = Q_m + Q_f$ would be lowered or even totally ignored depending on whether or not the entire deviation from stoichiometry is accommodated by the intrinsic vacancies. Therefore, β'-AuZn falls in the class of β'-AuCd,[5] CoAl,[27] and NiAl,[28] etc., where a vacancy-defect structure is known to exist in the Cd- and Al-rich sides only.

The result appears contrary to the earlier thinking[5] that when there is an appreciable difference between the atomic size of the constituent species of a CsCl-type alloy, the vacancy-defect structure is likely to exist on the sublattice occupied by the species having smaller atomic size. In the present case of β'-AuZn, the atomic size of Au and Zn atoms are, respectively, 2.88×10^{-8} and 2.76×10^{-8} cm, the atomic-size difference being very small, only 6%, and that too in the reverse sense as compared with β'-AuCd, CoAl, and NiAl, etc. Therefore, only substitutional defects were expected on both sides of equiatomic AuZn composition. Perhaps, valence effects rather than the relative size brings about the creation of vacancy-defect structures in such a manner that the e/a ratio of $\frac{3}{2}$ is not exceeded in these Hume-Rothery's compounds.

C. Preexponential Factors D_0 and Correlation Factor f

The parallelism between Q and $\log D_0$ in Fig. 6 suggests that these quantities are related to each other. Use may be made of Wert and Zener's relationship[29] for the entropy of activation:

$$\Delta S = \lambda \beta Q / T_m , \tag{7}$$

where λ is an empirical constant of the order of 1.0 in bcc metals, $\beta = -d \log_{10} \mu / d(T/T_m)$ is the experimentally measured temperature dependence of the elastic shear modulus μ, Q is the measured diffusional activation energy, and T_m the melting temperature in degrees Kelvin. If (7) is substituted in (2), then

$$D_0 = \gamma a^2 \bar{\nu} f e^{\lambda \beta Q / R T_m} . \tag{8}$$

Taking $\bar{\nu} \simeq \nu_D$ the Debye frequency, a plot of $\ln(D_0/a^2 \nu_D)$ vs $\lambda \beta Q / R T_m$ should be linear with an intercept of $\ln f$ since $\gamma = 1$. In the absence of data on the temperature dependence of the elastic constants [β in Eq. (8)] in β'-AuZn, a plot of $\ln(D_0/a^2 \nu_D)$ vs Q/RT_m is appropriate since only the relative value of the

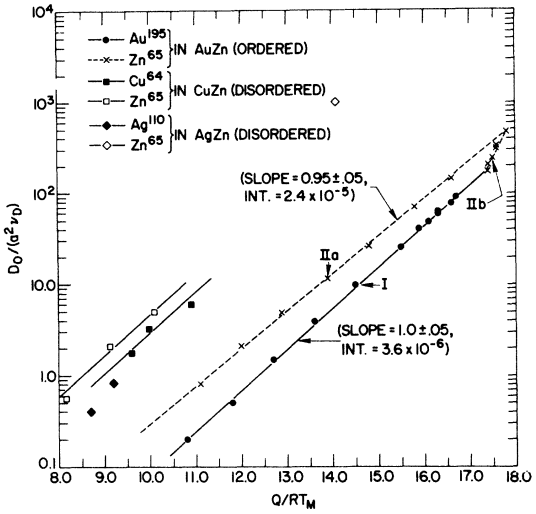

FIG. 7. Relationship between normalized frequency factors ($D_0/\alpha^2\nu_D$) and activation energies (Q/RT_m) in ordered β'-AuZn, and disordered β-CuZn and β-AgZn.

intercept is of interest. In that event, Eq. (8) reduces to the empirical relationship of Dienes[30]

$$(D_0/a^2\nu_D) = K e^{Q/RT_m}, \tag{9}$$

where K is the intercept now $\sim 10^{-6}$ and the slope is 1. It may be remarked that the subsequent papers on this subject, notably by LeClaire[31] and Buffington and Cohen, [32] merely elucidate Dienes's empiricism on the bases of thermodynamics and an elastic model, but Eqs. (8) and (9) remain materially unaffected.

The Debye frequency in β'-AuZn, equal to 4.1×10^{12} and relatively insensitive to composition, was computed from the respective Θ values of the constituent species according to the procedure of Passaglia and Love. [33] Data on the lattice parameters and melting points were taken from Muldawar[34] and Hansen, [14] respectively. The plots of normalized activation energies for diffusion Q/RT_m vs $\ln(D_0/a^2\nu_D)$ for Au^{195} and Zn^{65} tracers are shown in Fig. 7. The data for Au^{195} tracer (curve I) fit extremely well on a straight line with a slope of 1.00 ± 0.05 and intercept of 3.6×10^{-6}. Obviously, whenever the enthalpy of activation ($\Delta H \sim Q$) changes there is a corresponding change in the entropy of activation as well. Thus, it is the Gibb's free energy $\Delta G = \Delta G_f + \Delta G_m$ for the diffusion process which brings about the one to one change in Q and D_0 seen in Fig. 6. Any perturbation in ΔG_f (for example, the presence of a vacancy-defect structure) and/or ΔG_m (e.g., kinetics of HME loops on the basis of the quasichemical model[20]) affects both Q and D_0 equally, and, consequently, the two parameters may be considered conjugate.

The data for Zn^{65}, however, are divided into two distinct regions indicated by II(a) and II(b) in Fig. 7; the former shows a reasonable straightline fit with a slope of 0.95 ± 0.05 and intercept of 2.4×10^{-5}. It may be noted that while the points on curves II(a) and II(b) maintain the same compositional sequence as in Fig. 5, showing a systematic decrease of Zn content in the alloys going from left to right, no such composition identity exists for the Au points on curve I. The splitting of the Zn^{65}-tracer data along the curves II(a) and II(b) and their level with respect to the Au^{195} data on curve I constitutes *direct* evidence of the presence of vacancy-defect structure in the Zn-rich side of β'-AuZn alloys. Considering only the temperature-independent part of Eq. (3), the ratio of frequency factors may be written

$$G_0 = \frac{D_0(\mathrm{Zn})}{D_0(\mathrm{Au})} = \frac{n+2}{2n+1}, \tag{10}$$

where as before $\bar{\nu}_{Zn} \sim \bar{\nu}_{Au}$ and $n_{Zn}/n_{Au} = n$. When $n \ll 1$ (that is, the vacancy-defect structure is predominant), $G_0 \to 2$, which explains the reason for the displacement of Zn^{65} data [line II(a)] from Au^{195} data (line I) by a factor of about 2. As the composition of the alloy changes to the Au-rich side of the 50 : 50 composition, the vacancy-defect structure degenerates into antistructure defects, vacancies from the Au sublattice are elimated, and $G_0 \to \sim 1$. In Fig. 7, the data along II(b), where all the points are in the Au-rich side, very rapidly drops to the level of the Au^{195} diffusion along line I. The frequency factor "equalization" where $G_0 = 1$ is the point where II(b) meets I and, of course, can only happen in the Au-rich side. Hence this situation also accounts for the absence of "cusps" in Zn^{65} diffusivities since D_{Zn} must always drop until "equalization" occurs and should simply level off if only antistructure defects are present in the Au-rich side.

The intercept in Fig. 7 should be controlled primarily by the correlation factor f in the disordered and ordered phases. Fishman *et al.* [10] reported from their study of the isotope effect in equiatomic FeCo that $f_{(\mathrm{ordered})} \to (f_{(\mathrm{disordered})})^6 \sim 0.12$, a change in f by a factor between 5 and 10. In the absence of a disordered β-AuZn phase, comparison was made between ordered β'-AuZn diffusion parameters and those in disordered β-CuZn[13,16,17] and β-AgZn. [18,19] Such an approach is not unreasonable since all three alloys are Zn base-monovalent systems. The values of ν_D in CuZn and AgZn were 7.0×10^{12} and 5.4×10^{12}, respectively[33]; the melting points[14] and the lattice parameters[35] were obtained from the literature. The normalized data for the above disordered alloys is also shown in Fig. 7. The Zn- and Cu-tracer diffusion points in β-CuZn show fair fit to the straight lines of slope 1.0 drawn

through them. While the data in the disordered β-AgZn show relatively large scatter, they also roughly follow the pattern of β-CuZn. The remarkable feature of Fig. 7 is that the data for the disordered phases are separated from that of the ordered β'-AuZn by about an order-of-magnitude change in the intercept indicating that f in the ordered AuZn phase, indeed, approaches zero.

V. CONCLUSIONS

This study provides further direct evidence that in highly ordered alloys, such as β'-AuZn (LRO = 0.96) examined here, the correlation factor f approaches zero. The conclusion is that the HME correlation six-jump cycle, in spite of its very low efficiency, is the only mechanism which permits net diffusion to take place while preserving the equilibrium degree of long-range order. It has been possible to infer the presence of a vacancy-defect structure in the Zn-rich side of the 50:50 AuZn composition from the observed ratios of diffusivities and invoking the six-jump-cycle diffusion mechanism.

ACKNOWLEDGMENTS

The authors wish to thank the U. S. Air Force Office of Scientific Research for partial support of this work and the U. S. Atomic Energy Commission for the use of facilities in the Materials Research Laboratory of the University of Illinois, Urbana-Champaign. Assistance of M. P. Austin in the laboratory and P. A. Roland (of IBM Research Center) in computations is also acknowledged. The continued interest and helpful comments of Dr. C. A. Wert, Dr. D. Lazarus, and Dr. M. G. Coleman during this investigation are appreciated.

---

*Supported in part by the U. S. Air Force Office of Scientific Research under Grant Nos. 900-65 and 68-1599; additional support was received from the U. S. Atomic Energy Commission through the use of technical facilities of the Materials Research Laboratory at the University of Illinois in Urbana-Champaign, Illinois, and the IBM Research Center, Yorktown Heights, N. Y.

†Present address: IBM Watson Research Center, Yorktown Heights, N. Y. 10598.

[1]See, e. g., D. Lazarus, Solid State Phys. 10, 71 (1960); N. L. Peterson, *ibid.* 22, 409 (1968).

[2]K. Compaan and Y. Haven, Trans. Faraday Soc. 54, 1498 (1958).

[3]A. B. Lidiard, Phys. Rev. 106, 823 (1957).

[4]E. W. Elcock and C. W. McCombie, Phys. Rev. 109, 605 (1958).

[5]D. Gupta, D. S. Lieberman, and D. Lazarus, Phys. Rev. 153, 863 (1967).

[6]H. B. Huntington, N. C. Miller, and V. Nerses, Acta Met. 9, 749 (1961).

[7]P. Wynblatt, Acta Met. 15, 1453 (1967).

[8]D. Gupta and D. S. Lieberman, *Ordered Alloys: Structural Applications and Physical Metallurgy* (Claitor, Baton Rouge, La., 1970), p. 195.

[9]E. W. Elcock, Proc. Phys. Soc. (London) 73, 250 (1959).

[10]S. G. Fishman, D. Gupta, and D. S. Lieberman, Phys. Rev. B 2, 1451 (1970).

[11]See, e. g., J. Mullen, Phys. Rev. 121, 1649 (1961); A. LeClaire, Phil. Mag. 14, 271 (1966).

[12]J. R. Beeler, Jr. and J. A. Delaney, Phys. Rev. 130, 962 (1963).

[13]A. B. Kuper, D. Lazarus, J. R. Manning, and C. T. Tomizuka, Phys. Rev. 104, 1536 (1956).

[14]M. Hansen and K. Anderko, *Constitution of Binary Alloys*, 2nd ed. (McGraw-Hill, New York, 1958).

[15]H. Iwasaki and Tomoko Uesugi, J. Phys. Soc. Japan 25, 1640 (1968).

[16]M. C. Inman, D. Johnston, W. L. Mercer, and R. Shuttleworth, in *Proceedings of the Second Radioisotopes Conference, Oxford*, 1954 (Butterworths, London, 1954), Vol. II, p. 85.

[17]A. B. Kuper and C. T. Tomizuka, Phys. Rev. 98, 244 (1955).

[18]P. P. Kuzmenko, E. K. Kharkov, and G. P. Grinevich, Zh. Ukrain Fiz. 5, 683 (1960).

[19]T. Heumann and P. Lohmann, Z. Elecktrochem. 59, 849 (1955).

[20]H. A. Domian and H. I. Aaronson, Trans. AIME 230, 44 (1964).

[21]W. C. Hagel and J. H. Westbrook, in *Diffusion in Body Centered Cubic Metals* (American Society for Metals, Metals Park, Ohio, 1965), p. 197; also H. A. Domian and H. I. Aaronson, *ibid.*, p. 209.

[22]Au was obtained from Sigmund Cohn Co. and Zn from American Smelting and Refining Co.

[23]Analyses for Au content of the alloys were carried out by Lucius Pitkin Inc., New York, N. Y.

[24]Au^{195} and Zn^{65} isotopes were obtained from Nuclear Science and Engineering Corp., Pittsburgh, Pa.

[25]Density measurements were made by the water-displacement method at room temperature to a precision of $\pm 5\times10^{-4}$.

[26]A. C. Damask and G. J. Dienes, *Point Defects in Metals* (Gordon and Breach, New York, 1963), p. 195.

[27]A. J. Bradley and G. C. Seager, J. Inst. Metals 64, 81 (1939).

[28]A. J. Bradley and A. Taylor, Proc. Roy. Soc. (London) A159, 56 (1937).

[29]C. Wert and C. Zener, Phys. Rev. 76, 1169 (1949).

[30]G. J. Dienes, J. Appl. Phys. 21, 1189 (1950).

[31]A. D. LeClaire, Acta Met. 1, 438 (1953).

[32]F. S. Buffington and M. Cohen, Acta Met. 2, 660 (1954).

[33]E. Passaglia and W. F. Love, Phys. Rev. 98, 1006 (1955). Average value based on Debye characteristic Θ values for Zn, Au, Cu, and Ag at 325.1, 161.6, 345.3, and 225.4 °K, respectively. The average Θ for the alloy was computed by the formula $1/\Theta_{av}^3 = (1-x)/\Theta_A^3 + x/\Theta_B^3$, where A and B are the alloy constituents and x is the mole fraction.

[34]Leonard Muldawer (private communication), actual values in 48.1, 50.8, and 51.9 at.% Zn alloys being 3.1530, 3.1485, 3.1470, and 3.1466 Å, respectively.

[35]W. B. Pearson, *Handbook of Lattice Spacings and Structure of Metals* (Pergamon, New York, 1967), Vol. II.